Supporting Information

Tunable nanoplasmonic mirror at electrochemical interface

Ye Ma[1], Cristian Zagar[1], Daniel J. Klemme[2], Debabrata Sikdar[1,3], Leonora Velleman[1], Yunuen Montelongo[1], Sang-Hyun Oh[2], Anthony R. Kucernak[1], Joshua B. Edel[1], Alexei A. Kornyshev[1]

[1]Department of Chemistry, Imperial College London, SW7 2AZ, United Kingdom
[2]Department of Electrical and Computer Engineering, University of Minnesota, Minneapolis, Minnesota, 55455, USA.
[3]Department of Electronics and Electrical Engineering, Indian Institute of Technology Guwahati, Guwahati-781039, India

1. Diameter of nanoparticles

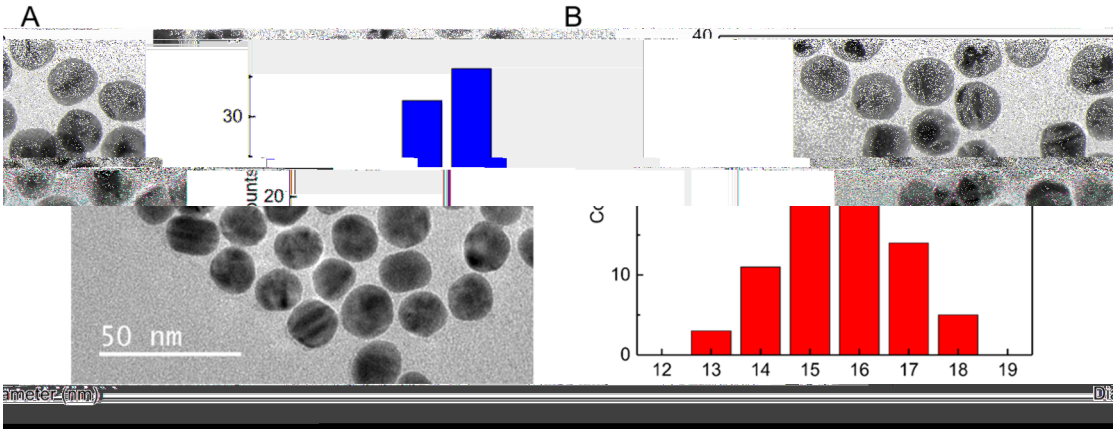

Figure S1 Diameter of NPs. A. TEM image of as prepared NPs. B. Statistics of the measured diameters of NPs.

2. Stability of nanoparticles

Since the NPs are covered by negatively charged carboxylic ligands, the pH and salt concentration directly influence the surface charge density on NPs and the electrolyte screening of these charges, respectively, which both determine the stability of the NP solution.

Agglomeration of NPs has a signature in bulk light-absorption spectra, in the form of the appearance of a shoulder in the orange/red part of the spectrum. As shown in the Figure S2A, with increasing pH, the typical shoulders for aggregation of NPs at around 600 nm disappear, indicating that higher pH does increase the stability of NPs. Above pH 6.2, NPs were found to be able to tolerate electrolyte concentration as high as 60 mM NaCl. At the same time, according to our calculation, at pH 6.2, 96% MDDA are already dissociated (leading to about 1050 negative charges on each of our 16 nm NPs). Thus, further increase of pH would not make much difference regarding the stability of NPs. This was experimentally confirmed by comparing the stability of NP-dispersions with respect to salt concentration at pH 6.2 and pH 7.1: both can tolerate 80 mM solution, as an upper limit for electrolyte concentration (Figures S2B and C). Therefore, we use pH 6.2 in all experiments. Such well stabilized NP solution can tolerate a wide range of NaCl concentrations and gives us more freedom for the control of the switching process.

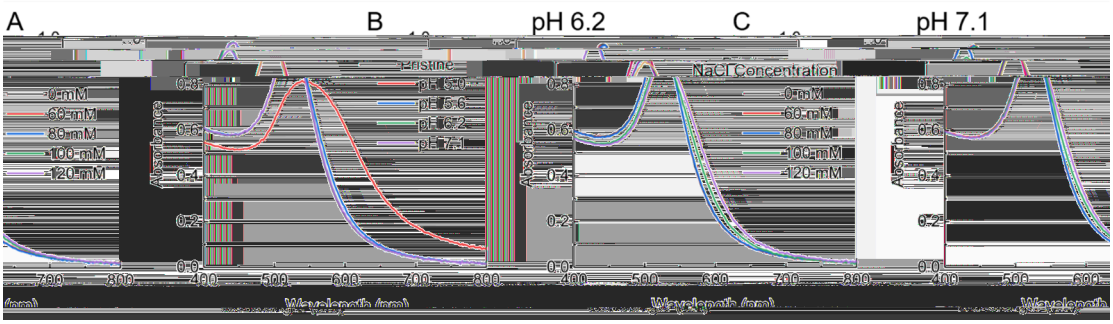

Figure S2 Stability of NP solution. A. UV-vis spectra of NP solution with 60 mM NaCl at different pH and pristine as-prepared NP solution as the reference. B. UV-vis spectra of NP solution at pH 6.2 with different concentration of NaCl. C. UV-vis spectra of NP solution at pH 7.1 with different concentration of NaCl.

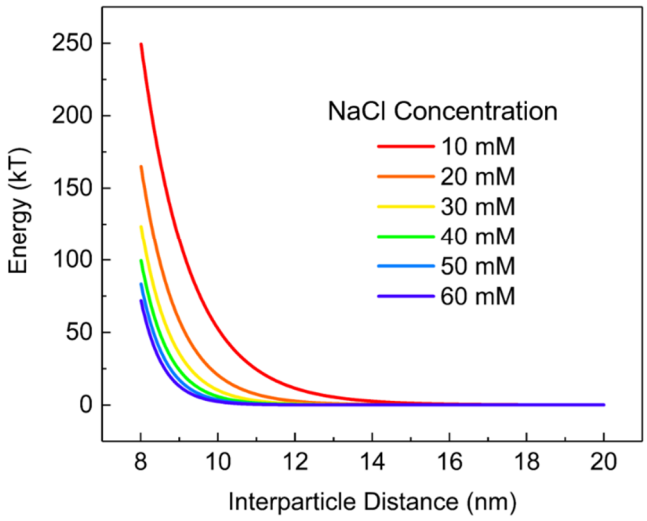

Figure S3 Energy profiles of NP pair in different concentration of NaCl

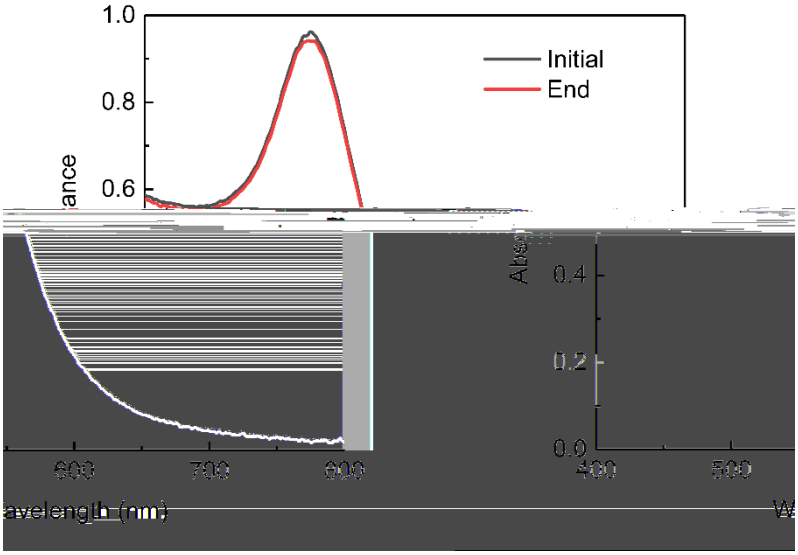

Figure S4 UV-vis spectra of NP solution before and after the reversibility experiment.

3. Estimation of surface charge on MDDA functionalized gold NPs

For a NP of 16 nm diameter, the surface area is 804 nm^2. Given the number of MDDA molecules during the synthesis is excess to that needed for the full coverage of NP surface, and the packing density of the MDDA is 1.333 per nm^2, one can estimate the number of MDDA on the single NP as about 1100 molecules.[1] Assuming the adsorbed and the drifting MDDA to have the same pKa, we then can come up with the following equations:

$$pK_a = -log_{10}\left(\frac{[MDD^-][H^+]}{[MDDA]_{initial} - [MDD^-]}\right) = pH + log_{10}\left(\frac{[MDDA]_{initial}}{[MDD^-]} - 1\right) \quad (SI-1)$$

$$\frac{1}{10^{(pK_a - pH)} + 1} = \frac{[MDD^-]}{[MDDA]_{initial}} \quad (SI-2)$$

where $MDDA_{initial}$ is the total amount of MDDA present in all forms and MDD^- is the disassociated form which carries one negative charge on each molecule. Since the pKa of MDDA is about 4.8 and the pH we are operating with is 6.2, the disassociation ratio would be 0.96. Thus, the total negative charges on single NP is about 1050.

4. Five-layer Stack model for reflection spectra

The five-layer stack model used for calculation of optical reflectance spectra of the system under study is described in detail below. In order, light interacts with the electrolyte solution (medium 1), nanoparticle array (medium 2), medium 3 located between the array and interface (can be also electrolyte or a layer of ligands, acting as 'spacer' layer), and the conductive film (medium 4) coating the semi-infinite electrode (medium 5). This structure is sketched in Figure 7, where d, h_s and h_f are the thicknesses of the layer representing the NP array, the spacer, and the coating film, respectively; a is the centre-to-centre separation between NPs. For each layer, dielectric constants are labelled as ϵ_1, ϵ_2, $\epsilon_3 \equiv \epsilon_1$, ϵ_4 and ϵ_5.

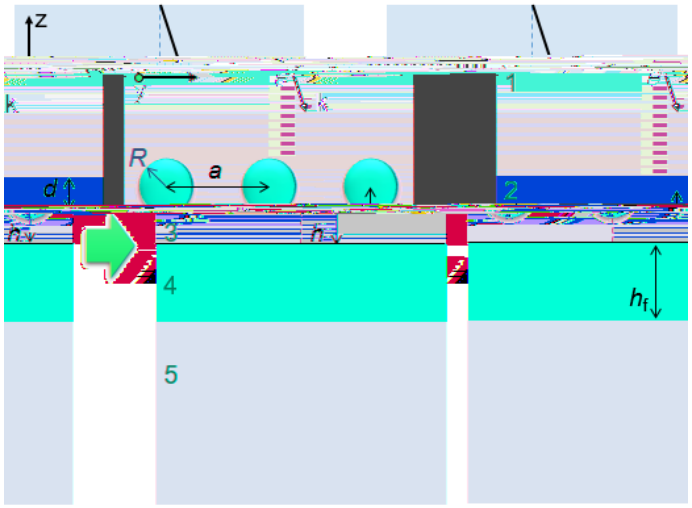

Figure S5 Schematic representation of a nanoparticle 'mirror-on-mirror' system and its corresponding 5-layer stack model, introduced in Ref.[2]

As described in Ref.[2] when the wavelength of incident light is much larger compared to the NP radii (all NPs assumed to be of the same size), the effective polarizability of an NP in the film representing the array of NPs, in the parallel and perpendicular directions with respect to the film, respectively, is, given by:

$$\beta_{\parallel}(\omega) = \frac{\alpha(\omega)}{1 + \alpha(\omega)\frac{1}{\epsilon_1}\left[-\frac{1}{2}\frac{U_A}{a^3} + \xi(\omega)\left(\frac{f(h,a)}{a^3} - \frac{3}{2}\frac{g_1(h,a)}{a^3} + \frac{1}{8h^3}\right)\right]} \qquad (SI-3)$$

$$\beta_{\perp}(\omega) = \frac{\alpha(\omega)}{1 + \alpha(\omega)\frac{1}{\epsilon_1}\left[\frac{U_A}{a^3} - \xi(\omega)\left(\frac{f(h,a)}{a^3} - 12\frac{h^2 g_2(h,a)}{a^5} - \frac{1}{4h^3}\right)\right]} \qquad (SI-4)$$

The function $\alpha(\omega)$, in the expressions above, is the isotropic polarizability of a free particle immersed in medium 1 (in the absence of boundaries with other dielectric media or NPs), which can be written in terms of the dielectric constant of NP, ϵ_{NP} (essentially, of the material of NPs but with NP-size dependent correction), and the NP radius, R:

$$\alpha(\omega) = \epsilon_1 R^3 \frac{\epsilon_{NP} - \epsilon_1}{\epsilon_{NP} + 2\epsilon_1} \qquad (SI-5)$$

The effective polarizabilities $\beta_{\parallel}(\omega)$ and $\beta_{\perp}(\omega)$contain contributions from both the interactions with other NPs in the array and the images of the effective dipoles emerging due to excitation of localized plasmons. The constant U_A is determined by the geometry of the array; the term containing it accounts for the interaction between NPs. For a hexagonal lattice, $U_A = 11.031$. The other contributions come not only from the images of all the other particles (terms proportional to $f(h,a)$, $g_1(h,a)$ and $g_2(h,a)$), but also from its own image, represented by the term proportional to $\frac{1}{h^3}$. Naturally, to get the correct magnitude of the images in a multilayer system, the image charge factor, $\xi(\omega)$, should be properly calculated. For our purposes this can be simplified to the image emerging at the interface of media 1 and 4 (hereafter we consider for simplicity the optical dielectric properties of media 1 and 3 to be the same), thus giving:

$$\xi(\omega) = \frac{\epsilon_1 - \epsilon_4(\omega)}{\epsilon_1 + \epsilon_4(\omega)} \qquad (SI-6)$$

From the polarizabilities, $\beta_{\parallel}(\omega)$ and $\beta_{\perp}(\omega)$, one can calculate the effective in plane and normal dielectric constants of the layer representing the NP array:

$$\epsilon_2^{\parallel}(\omega) = \epsilon_1 + \frac{4\pi}{a^2 d}\beta_{\parallel}(\omega) \qquad (SI-7)$$

$$\frac{1}{\epsilon_2^{\perp}(\omega)} = \frac{1}{\epsilon_1} - \frac{1}{\epsilon_1^2}\frac{4\pi}{a^2 d}\beta_{\perp}(\omega) \qquad (SI-8)$$

After modelling all dielectric constants in the system, the next step is to write a transfer matrix, $\widetilde{M}_n$, which depends upon reflection and transmission coefficients of the interface between layers n, and $n+1$.

$$\widetilde{M}_n = \frac{1}{t_{n,n+1}}\begin{pmatrix} e^{-i\delta_{n+1}} & r_{n,n+1}e^{i\delta_{n+1}} \\ r_{n,n+1}e^{-i\delta_{n+1}} & e^{i\delta_{n+1}} \end{pmatrix} \qquad (SI-9)$$

In the expression above, δ_{n+1} represents the phase difference between the reflected beams in layer n: the one reflected directly by the interface between layers n and $n+1$, and the one reflected by the interface between $n+1$ and $n+2$.

The total transfer matrix of the system is given by the product of the individual transfer matrices of each interface.

$$\widetilde{M} = \widetilde{M}_1\widetilde{M}_2\widetilde{M}_3\widetilde{M}_4 \qquad (SI-10)$$

The total reflection coefficient is then expressed through the elements of the total transfer matrix, as

$$\tilde{r} = \frac{\widetilde{M}_{21}}{\widetilde{M}_{11}}, \qquad (SI-11)$$

This finally gives the reflectance of the system as,

$$R = |\tilde{r}|^2 \qquad (SI-12)$$

Transmittance can also be calculated in a similar way.[2]

5. Influence of the deviation of interparticle distance to the theoretical reflectance spectra

From our previous X-ray diffraction data of NPs at liquid-liquid interface[3], the standard deviation (std) ranged from 0.2 to 1.4 for an interparticle distance ~10.5 nm. As can be seen from Figure S6, there is negligible reflectance difference among std=0, 1, 2, indicating that the reflectance is not very sensitive to the deviations from uniform particle distribution.

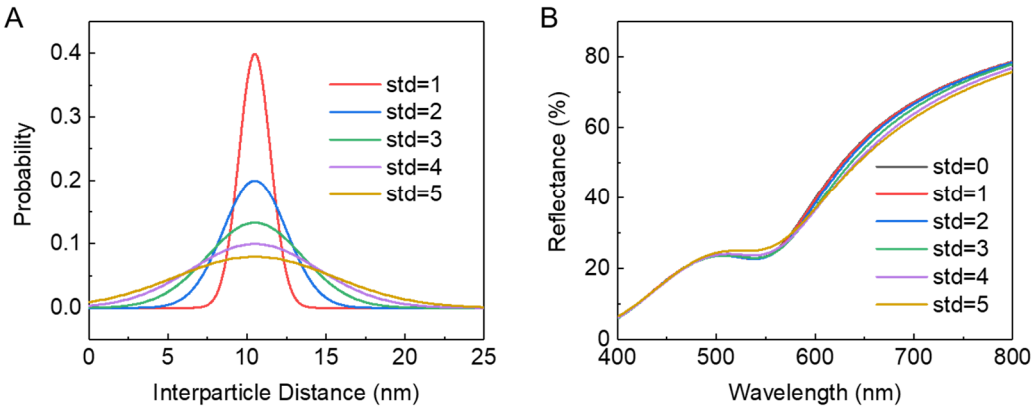

Figure S6 A. The Gaussian distributions of interparticle distance with different standard deviations (std). B. The calculated theoretical reflectance spectra considering the deviation of the interparticle distances from panel A.

The model behind this conclusion is based on averaging the theoretical reflectance signal (as function of interparticle spacing) over the normal distributions shown in Figure SI-6A. The results in Figure S6B are, therefore, described by the following equation[1, 3]:

$$R_{eff}(s_{avg},\sigma) = \int_{-\infty}^{\infty} \frac{\exp\left(-\frac{(s-s_{avg})^2}{2\sigma^2}\right)}{\sigma\sqrt{2\pi}} R(s)\, ds \qquad (SI-13)$$

where s is the centre-to-centre interparticle spacing, s_{avg} is its mean value, σ is the standard deviation of the separation distribution and $R(s)$ is the reflectance for the given s value.

6. Geometric conversion of inter-particle distance into coverage

To calculate coverage geometrically, one should go to its definition, as number of particles per unit area. In a triangular lattice, as shown in figure SI-6), each particle is surrounded by six others. The particle in the centre is divided equally between six equilateral triangles, so each corner of each triangle contains 1/6 of a particle. In other words, half a particle per triangle. This number, 0.5, is then divided by the area of the triangle. Introducing the notations a for surface-to-surface separation between particles and R for nanoparticle radius, the coverage becomes:

$$\Gamma = \frac{0.5}{(2R+a)^2\frac{\sqrt{3}}{4}} = \frac{2}{\sqrt{3}(2R+a)^2} \qquad (SI-14)$$

Maximum coverage is attained when particles are tangent to each other, when $a = 0$.

$$\Gamma_m = \frac{1}{2\sqrt{3}R^2} \qquad (SI-15)$$

Plugging in the value for the nanoparticle radius $R = 8.25$ nm leads to $\Gamma_m = 4.24 \cdot 10^{11}$ cm^{-2}.

From eq. S13 and S14, the fractional coverage can be written as:

$$\theta = \frac{\Gamma}{\Gamma_m} = \left(\frac{2R}{2R + a}\right)^2 \qquad (SI - 16)$$

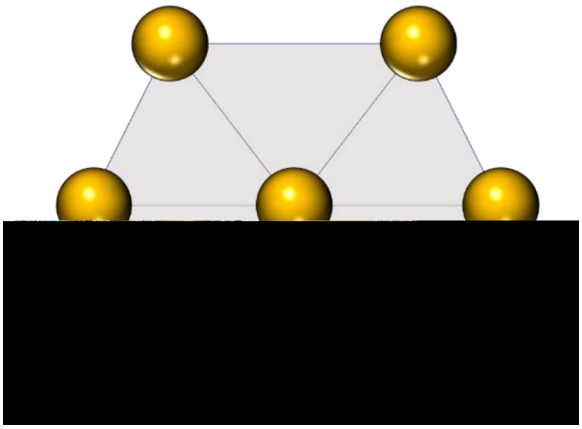

Figure S7 Representation of a hexagonal NP lattice

7. The Presence of the energy barrier at the SLI

During examining the NP assembly process at the current solid-liquid interface, we found the sugnature of a free energy barrier. To clarify this, the plot of the square of the fractional coverage (θ^2) vs. time is shown below. It can be easily seen that at the beginning, within 3000 s the dependence is not linear (namely the coverage does not grow with time square-root-wise), indicating that the assembly is not simply diffusion-controlled process. In fact, the behaviour of the curve there is closer to parabolic, which would translate into a linear dependence between θ and t, implying the presence of a potential barrier.[4] The trend to saturation of the surface at longer times (after 6000 s) is also seen (in that range the plot should not be linear either). Therefore, it is strategically better to use the full diffusion-influenced adsorption model[4] in order to approximate the whole profile, since it leads to the more solid conclusion: both adsorption and desorption count.

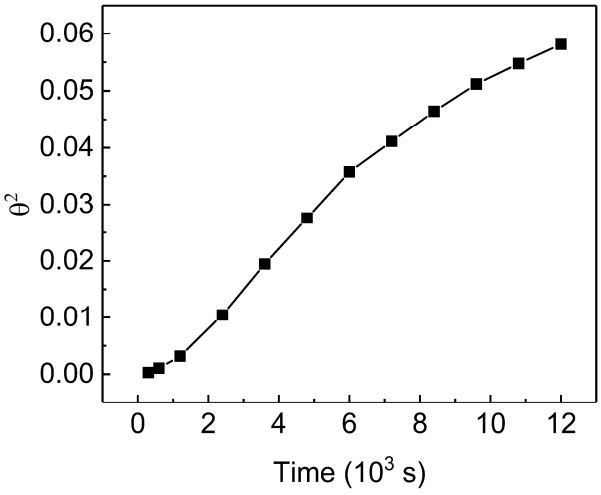

Figure S8 The square of the fractional coverage (θ^2) vs. time in 60 mM NaCl solution.

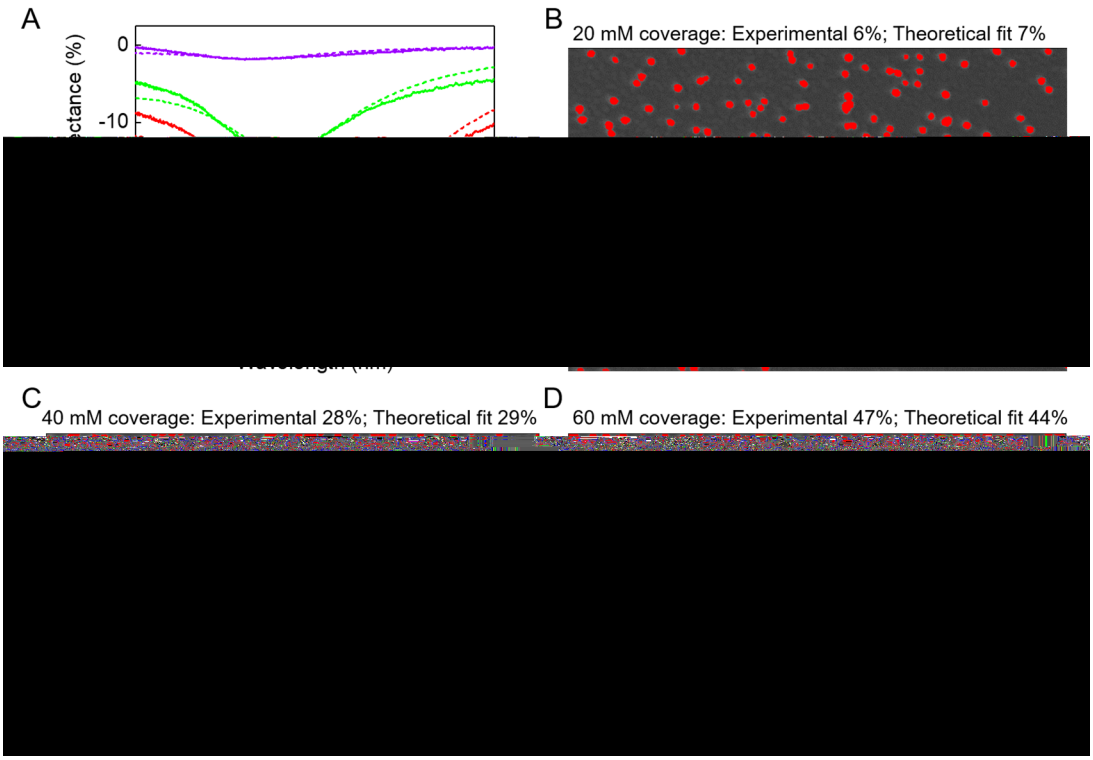

Figure S10 Comparing the NP coverages calculated from SEM and EMT. A. Experimental (solid) and theoretically fitted (dashed) curves of the change in reflectance of NPs/TiN/Ag for different NaCl concentrations after drying, with respect to the pristine TiN/Ag substrate. B, C and D are the SEM images for different dried NPs/TiN/Ag samples with red- pseudo-coloured NPs for calculating NP coverages, scale bar 100 nm.

References:

(1) Montelongo, Y.; Sikdar, D.; Ma, Y.; McIntosh, A. J. S.; Velleman, L.; Kucernak, Anthony R.; Edel, J. B.; Kornyshev, A. A., Electrotunable Nanoplasmonic Liquid Mirror. *Nat. Mater.* **2017**, *16*, 1127.

(2) Sikdar, D.; Hasan, S. B.; Urbakh, M.; Edel, J. B.; Kornyshev, A. A., Unravelling the Optical Responses of Nanoplasmonic Mirror-on-Mirror Metamaterials. *Phys. Chem. Chem. Phys.* **2016**, *18*, 20486-20498.

(3) Velleman, L.; Sikdar, D.; Turek, V. A.; Kucernak, A. R.; Roser, S. J.; Kornyshev, A. A.; Edel, J. B., Tuneable 2d Self-Assembly of Plasmonic Nanoparticles at Liquid|Liquid Interfaces. *Nanoscale* **2016**, *8*, 19229-19241.

(4) Miura, T.; Seki, K., Diffusion Influenced Adsorption Kinetics. *J. Phys. Chem. B* **2015**, *119*, 10954-10961.